Enhancing 5G Data Transmission Through Sub-Carrier Spacing Optimization

Abhijit Boruah[1], Rabinder kr. Prasad[1], N. Hemarjit Singh[2], Abhijit Biswas[3] and Sudipta Majumder[1*]

[1]Department of CSE, DUIET, Dibrugarh University, Assam, India
[2]Department of ECE, DUIET, Dibrugarh University, Assam, India
[3]Department of CSE, Assam University, Assam, India

*Corresponding Email: sudipta2020@dibru.ac.in

Received April 13, 2024, Revised June 24, 2024, Accepted July 9, 2024, Published December 16, 2024

Abstract. *5G networks can support various UDP and TCP applications. Efficient and reliable 5G network performance offers faster speeds, improved connectivity, and the capability to manage multiple applications across different locations. This study comprehensively analyses the effect of various subcarrier spacing (SCS) scenarios of 5G networks on the performance of smartphones, cameras, and sensors. The analysis shows that higher SCS values are associated with increased average throughput. It indicates that higher subcarrier spacing values enable more efficient data transmission. Smartphones have low and symmetrical jitter with numerology values of 3 and 2, making them well-suited for bidirectional communication. In comparison, cameras are more efficient than sensors at delivering data with a lower delay at all SCS values, which is crucial for applications requiring fast response times. We propose an adaptive Q-learning-based algorithm that automatically adjusts (SCS) configurations based on real-time network conditions and application needs. This approach significantly enhances network performance across various scenarios. The findings of this study have significant implications for the design and implementation of 5 G networks, as they provide insights into the optimal SCS settings for applications with specific requirements and priorities, thereby guiding network engineers and professionals in their decision-making process.*

Keywords:
5G, subcarrier spacing, throughput, delay, jitter, q-learn-ing

1. Introduction

The success of the foundation for fifth-generation (5G) New Radio (NR) hinges on its adaptability to a variety of frequency ranges and scenarios [1-2]. NR defines a set of numerologies or sub-carrier spacing that can work with numerous frequency bands and deployment schemes [1]. Both a cyclic prefix overhead and a sub-carrier spacing are included in these numerologies. This adaptability of the 5G network instils a sense of reassurance in the audience that it can handle a wide range of scenarios. In the early phases of the 5G standard, single-carrier schemes, such as single-carrier frequency division multiple access (SC-FDMA), were utilized. In subsequent releases of the standard, they were eventually replaced by other multiple access schemes, such as orthogonal frequency division multiple access (OFDMA) and non-orthogonal multiple access (NOMA) [3].

For several reasons, single-carrier schemes are less prevalent in 5G than in previous wireless communication standards. Single-carrier schemes are more susceptible to frequency-selective fading, reducing signal quality and dependability in specific frequency bands. In contrast, OFDMA and NOMA are more resistant to frequency-selective fading due to their dynamic subcarriers and power allocation [4]. Single-carrier schemes are less efficient in terms of spectral efficiency than OFDMA and NOMA [5], which is another reason why they are less extensively utilized in 5G. OFDMA and NOMA make more efficient use of the available frequency spectrum by dividing it into multiple subcarriers and dynamically allocating them to users according to their channel conditions and quality of service requirements [6-7]. Choosing an SCS for gNB operation under full buffer

conditions theoretically involves a trade-off between latency and throughput at the physical (PHY) layer [8].

Numerous studies have focused on optimizing SCS for 5G networks. For instance, [9] highlights that while network slicing enables each slice to be optimally configured in terms of packet scheduler and numerology to meet specific service requirements, it can result in limited trunking gains compared to non-sliced scenarios. Similarly, [10] introduced novel resource scheduling and allocation techniques to mitigate inter-numerology leakage and optimize SCS performance. However, these techniques can lead to increased computational overhead, resource allocation challenges, and potential interference between numerologies. In [11], adaptive numerology selects the optimal numerology configuration based on Quality of Service (QoS) requirements and channel conditions. Despite its potential, the algorithm necessitates real-time analysis of multiple channel parameters and QoS metrics, which may introduce overhead and computational burdens on the system. Additionally, [12] discusses optimizing mixed numerology profiles for 5G wireless communication scenarios by introducing an optimization model that plans numerology profiles based on traffic needs and impairments. Nonetheless, this proposed system model is prone to various challenges, such as inter-numerology interference and low spectral efficiency. Moreover, previous studies have been limited in scope as they needed to consider parameters such as throughput, delay, and jitter and implement realistic experimental setups.

This study aims to assess the impact of sub-carrier spacing on 5G network performance. By utilizing an adaptive machine learning algorithm for SCS Optimization, this research seeks to provide insights that will enable informed decision-making to enhance the performance of 5G networks based on specific application needs and priorities. The study focuses on optimizing SCS, a crucial parameter in 5G networks, significantly impacting throughput, delay, and jitter. Different SCS values offer insights into enhancing network performance, including better handling of QoS requirements and channel conditions for more efficient and reliable 5G communications. By utilizing adaptive machine learning algorithms, the research allows for real-time adjustments, showcasing the potential of AI in network management. The study evaluates key performance metrics such as throughput, delay, and jitter, providing a comprehensive understanding of SCS adjustments' practical implications. The paper addresses research gaps by considering realistic experimental setups and often overlooked parameters, contributing to a holistic understanding of 5G optimization. The findings have wide-ranging applications, from high-speed data transfer to latency-sensitive uses like autonomous driving and real-time video communication, making the research relevant for industry and academia. It offers valuable guidance for future research, development, and designing robust 5G networks, as well as influencing standards and policies.

We have provided a brief introduction in this section. The remaining research article is divided into several sections. Section 2 provides the background of this work. Section 3 is a literature review where we have presented the related work conducted by other researchers. These studies shed light on various steps taken to optimize the performance of the 5G network. The materials and methodology are described in section 4, while section 5 reports the discussions of the experimental results. Finally, the logical conclusion and the scope of future work are provided in section 6.

2. Background

Optimizing the sub-carrier spacing in 5G mmWave networks is a critical factor that significantly affects these high-frequency communication systems' overall performance and efficiency. Optimizing the sub-carrier spacing is crucial for efficiently using the available spectrum, achieving maximum data speeds, reducing interference, and improving the quality of service [13]. 5G mmWave systems often use massive antenna arrays and beamforming techniques. Optimizing sub-carrier spacing is crucial for enabling efficient communication [14]. Balancing the trade-off between spectral efficiency and signal quality is essential when optimizing sub-carrier spacing. Operators can balance high data rates and reliable signal transmission by strategically adjusting the spacing between sub-carriers. This is particularly important in situations with significant interference and route loss, common in mmWave frequencies [15]. The optimization technique is essential in mmWave cloud radio access network (CRAN) deployments, where precise multi-lateration and exact positioning are necessary to ensure uninterrupted communication [16].

Moreover, the utilization of sub-carrier spacing optimization techniques in 5G mmWave networks is intricately connected to the development and execution of sophisticated beamforming technologies. Beamforming is a technique that includes manipulating and guiding radio signals towards particular users or places. Its effectiveness depends on carefully distributing sub-carriers for the best performance [17]. Optimizing sub-carrier spacing is crucial for effective beamforming operations in the context of massive MIMO systems, which involve vast antenna arrays [14]. Optimizing the sub-carrier spacing in 5G mmWave networks is essential for effectively dealing with the specific issues presented by the propagation properties of mmWave frequencies. Because mmWave signals experience significant free space route loss, it is necessary to utilize massive antenna arrays and precise sub-carrier spacing to overcome these propagation limits and ensure dependable communication across short distances [18]. Furthermore, implementing sub-carrier spacing optimization techniques can effectively reduce the negative influence of route loss and fading effects frequently encountered in mmWave channels [19]. Optimizing the sub-carrier spacing in mmWave systems will significantly improve the performance of wearable devices and enable faster and more precise data processing in the context of edge computing and object identification applications in 5G networks [20]. By utilizing high-frequency mmWave carriers with optimized spacing between sub-carriers, edge computing applications can use enhanced data transfer speed and decreased delay, resulting in enhanced object identification capabilities in wearable devices [21].

3. Literature Review

To improve the performance of 5G networks, different parts of the network need to be improved so that the user experience, data speed, and efficiency are all better. This process involves using methods and strategies to improve the network's capacity, coverage, reliability, and latency to keep up with the growing needs of users and apps. The most important goals of optimizing 5G networks are:

- Increasing the speed and capacity of data transmission so that it can handle more data traffic and the growing number of devices that are linked [22–23]
- Lower Latency: Lessening the time it takes for data to move between devices and the network so that applications can work in real-time and be very responsive [24–26]
- Improved Coverage: Making sure that the network coverage is more extensive and consistent to serve both urban and rural areas well [27–28].
- Efficient spectrum utilization means using the radio frequency spectrum, including the higher frequency bands, to increase network speed and capacity [29–31].
- Minimized Interference: Using advanced methods to reduce interference with signals and improve network stability as a whole [32]
- Network Resilience: Making the network better able to handle high loads and keep working well during times and events with a lot of users [33–35]
- Quality of Service (QoS) Management: Putting traffic in order of importance and making sure that essential apps get the bandwidth and performance levels they need [36–38]

When the features mentioned above are constantly improved, 5G networks can deliver on their promises of faster speeds, better connectivity, and support for new apps in many fields, including mobile communications, autonomous vehicles, healthcare, and the Internet of Things (IoT). Spectral efficiency, channel estimation, and interference mitigation are all parts of 5G wireless communication systems that are tied to each other and work together. Each of these parts is vital to making 5G networks work as well as they can, especially regarding subcarrier spacing [39-40].

Understanding the balance between energy efficiency (EE) and spectral efficiency (SE) in cognitive cellular networks plays a crucial role in effectively designing and optimizing such systems. In a study referenced as [41], researchers studied the trade-off between EE and SE in cognitive cellular networks. The research presented illustrative examples highlighting how the analysis of EE-SE trade-offs provided valuable insights and practical design guidelines for the upcoming generation of cognitive cellular networks. Researchers in [42] have implemented Sparse Code Multiple Access (SCMA), Polar codes, and Filtered OFDM (f-OFDM) as 5G enabling technologies that led to a notable enhancement in spectral efficiency. Field studies conducted by NTT DOCOMO and HUAWEI demonstrated that these technologies

improved spectrum efficiency by over 100% compared to the baseline technology of OFDMA and Turbo coding utilized in LTE.

The study in [43] shows that the better spectral efficiency of NOMA makes it a perfect candidate for 5G radio access because of its efficient spectrum use. So far, NOMA has been investigated from many different angles, including how resources are used and how fair things are. NOMA is also suitable for SISO (single input, Single Output) systems; it can also be used in MIMO (Multiple Input, Multiple Input) systems to make them even more powerful. NOMA can also be used in other communication systems, such as mmWave and visible light. The subcarrier spacing greatly affects the accuracy of channel prediction and estimation. Smaller subcarrier spacing offers finer frequency resolution, which makes it easier to get a more accurate estimate of the frequency response of a wireless channel.

The authors in [44] propose a new channel estimation approach using deep learning, which can be combined with least squares estimation (LSE). While LSE is low-cost, it results in high channel estimation errors. A MIMO system with a multi-path channel design simulates 5G networks, especially in situations with prominent Doppler effects. The study introduces a deep neural network with two examples, DNN-1 and DNN-2, to aid channel estimation in a MIMO-OFDM system under two different fading multi-path channel models based on the TDL-A model for 5G networks. The DNNs are trained using channel estimates from LSE and the corresponding ideal channels. Numerical results show that the proposed deep learning-assisted approach outperforms previous methods in terms of mean square error.

The study in [45] proposes a new deep learning-based architecture to enhance channel estimation using the least squares (LS) method. This approach employs a MIMO system with a multi-path channel profile for 5G-and-beyond network simulations, considering mobility effects indicated by Doppler shifts. The system model accommodates any number of transceiver antennas, and the machine learning module can utilize any neural network design. Numerical results demonstrate that the proposed deep learning framework outperforms traditional channel estimation methods. Among the neural network designs evaluated, bidirectional long short-term memory achieved the best channel estimation quality and the lowest bit error ratio. In [46], the researchers propose a deep learning approach using a multi-layer perceptron architecture that surpasses conventional CSI processing methods such as least square (LS) and linear minimum mean square error (LMMSE) estimation. This innovative technique opens up possibilities for a beyond fifth-generation (B5G) networking paradigm, where networking optimization is driven by machine learning. Unlike traditional estimation methods, this approach effectively handles large antenna arrays by simultaneously calculating the CSI of all pairwise channels using deep learning. The main focus is creating a learning architecture that can efficiently run on massively parallel platforms like GPU or FPGA.

The authors [47] addressed load balancing and interference reduction in heterogeneous networks with large MIMO macro cell base stations and wireless self-backhauling small cells. These small cell base stations, equipped with full-duplex transmission and regular antenna arrays, serve both macro and small cell users using the same frequency band for wireless backhaul. They reformulated the load balancing and interference reduction issue into a problem of maximizing network usefulness while considering wireless backhaul limitations. Using stochastic optimization, the problem was divided into dynamic scheduling of macro cell users, backhaul supply for small cells, and offloading macro cell users to small cells based on interference and backhaul links.

In the paper [48], the authors suggest a model-free multi-agent reinforcement learning (MARL) framework and a fully distributed self-learning interference mitigation (SLIM) scheme for autonomous networks. In SLIM, each small-cell base station (SBS) can determine what interferences are happening around it and how much power to send over the downlink without needing to communicate with other SBSs. To deal with the "dimensional disaster" of joint action in the multi-agent reinforcement learning (MARL) model, the authors used the Mean Field Theory to estimate the action value function. This dramatically reduces the amount of work that needs to be done on the computer. Simulation results based on the 3GPP dual-stripe urban model show that SLIM does a better job than many current interference coordination schemes at reducing interference, cutting

power use, and guaranteeing the quality of service for autonomous UDNs.

The OFDM system employed by NR access technology is flexible, allowing it to operate in a wide range of bands and supporting a wide range of deployment tactics, use cases, and methods of gaining access to the spectrum. Authors in [49] divide the spectrum into FR1 and FR2 bands to accommodate frequencies up to 52.6 GHz. FR1 operates at frequencies between 0.4 and 6 GHz, while mmWave frequencies in FR2 span 24.25 and 52.6 GHz. Although details are still lacking, NR Rel-16 will accommodate a broader range of frequencies [9]. Because of its flexible design, NR supports multiple sub-carrier spacings, each denoted by a unique Cyclic Prefix (CP) [22]. According to the numerical interval [0,4], the SCS is 15X2 kHz, and the slot length is [1/2] ms. Since larger SCSs are used at higher carrier frequencies, NR Rel-15 supports SCSs in the range of 15-240 kHz. In NR Rel-15, not all numerologies are allowed to be used with all physical channels and signals. For example, the numerology of 4 is not permitted to be used with data channels, and the numerology of 2 is not allowed with synchronization signals [8]. In addition, data channels in FR1 are limited to the digits 0 through 2, while those in FR2 can go up to three. Support for mmWave and higher frequencies is expected in NR Rel-16. Given that each physical resource block (PRB) in NR always contains 12 subcarriers, the width of each PRB is always equal to 180X2 kHz. The PRB width measures precisely this distance. Frames are 10 ms long and are split into 10 ms-long subframes so that they can be used with older versions of LTE. The number of slots in a subframe is 1/2, which is the numerology configuration because each slot contains 14 OFDM symbols. Without CP, an OFDM symbol takes 1/14X2 ms [49][50].

When numerology = 0, an LTE system is configured, but when it's more than 0, a wider bandwidth and a shorter Transmission Time Interval (TTI) are made possible, which is useful for mmWave bands and delay-critical services. NR can decrease the TTI and the access delay by allowing the SCS and OFDM symbol lengths to vary based on the configured numerology [51]. Three sub-types of numerology are used in 5G: numerology 1, 2, and 3. Each subtype has its own subcarrier spacing and symbol duration specifications. Numerology 1 is often utilized in 5G and is also known as regular cyclic prefix (CP) numerology. Its 15 kHz subcarrier spacing and 66.7-microsecond symbol duration make it appropriate for both uplink and downlink broadcasts. Numerology 2, also known as extended CP numerology, has a subcarrier spacing of 30 kHz and a symbol duration of 133.3 microseconds, greater than numerology 1. It is primarily intended for uplink transmissions and is typically used for low-power IoT devices and coverage enhancement [23]. Numerology 3, or short CP numerology, has a subcarrier spacing of 60 kHz and a symbol duration of 33.3 microseconds, which are both smaller than that of numerology 2. It is mainly used for downlink broadcasts and is designed to handle high-bandwidth applications such as virtual and augmented reality. Numerologies 1, 2, and 3 are utilized in 5G, each with its own subcarrier spacing and symbol duration [49]. According to the needs of the application and network conditions, these types of numerology are utilized to maximize data transmission over the air interface. Mini-slots and standalone slots are incorporated into NR with the numerologies to cut down on the time spent waiting for communication to occur [8]. Mini-slots are meant to reduce user latency by providing more leeway for the transmission of modest bits of data. Two OFDM symbols, each up to the slot's length, make up a mini-slot; one symbol may be in any frequency range, while the other must be 6 GHz or above. Slot formats are defined in [52], with slots being either completely Downlink (DL), completely Uplink (UL), or having both DL and UL components. To lessen delays, "self-contained slots" combine data and control functions into a single location. The time it takes for a signal to get from its source to its intended recipient can be decreased to achieve this goal. For instance, the ACK/NACK is scheduled alongside the DL data, or the UL transmission immediately follows the UL grant, all within the same period. These two instances share a time window [50].

An assessing performance matrix is a tool used to determine how well a system, process, or person is doing. In our case, it's the 5G network performance. The matrix has a set of metrics or key performance indicators (KPIs) that are used to measure different parts of the performance, such as throughput, delay, and jitter. An evaluating performance matrix is used to give a complete and objective performance re-

view and to find areas that need improvement. Using a performance matrix, organizations can set performance goals, keep track of their growth over time, and make decisions based on data to improve how they run.

1. The downlink average throughput for Smartphone

To evaluate the downlink average throughput for smartphones in a 5G network, one can use the following formula [43-45]:

$$DownlinkAvgThroughput = \frac{\left(\frac{TotalBytes\ \mathrm{Re}ceived}{TotalTime}\right)}{ChannelBandwidth} \quad (1)$$

(1) takes into account the total amount of data received by the device over the downlink channel during a specific period, the total time taken to receive the data, and the available bandwidth for the downlink channel. By using (1), one can obtain an estimate of the average downlink throughput for a smartphone in a 5G network. However, it is important to note that various factors, such as network congestion, signal strength, and interference, can affect actual downlink throughput.

2. Average delay evaluation formula for 5G mobile devices

Uplink average delay evaluation formula for 5G mobile devices is as follows [43-44].

$$UplinkAvgDelay = \frac{\sum\left(D_n - S_n\right)}{N} \quad (2)$$

Where:

- D_n is the time each uplink packet is received.
- S_n is the time when the nth uplink packet is sent. N denoted how many packets were delivered and received over the uplink.

The (2) formula calculates the amount of time that passes between a smartphone's uplink packet being delivered and the destination device receiving that packet.

The evaluation formula for the downlink average delay for smartphones in a 5G network is as follows [56-58].

$$DownlinkAvgDelay = \left(\frac{D_n - S_n}{n}\left(N\right)\right) \quad (3)$$

Where:

- D_n is the time that the nth downlink packet is received
- S_n is the time the nth downlink packet is transmitted.
- n is the number of data packets being sent
- N is the total number of downlink packets transmitted and received.

(3) adds up the time gap between each data packet being sent and received, then divides the result by the total number of data packets (n) and the number of users/devices (N) in the network. This shows the average transmission delay that each 5G smartphone has to deal with.

3. The average jitter for uplink and downlink smartphone

In a 5G network, the average jitter for uplink and downlink smartphone connections is calculated as follows [42-44]:

$$UplinkAvgJitter = \frac{SUM\left(UplinkPacketDelayVariation\right)}{NumberUplinkPacket} \quad (4)$$

$$DownlinkAvgJitter = \frac{SUM\left(DownlinkPacketDelayVariation\right)}{NumberDownlinkPacket} \quad (5)$$

Where:

- UplinkPacketDelayVariation is the difference between the average uplink packet delay and the delay of a single uplink packet.
- DownlinkPacketDelayVariance is the difference between individual downlink packet delays and the mean delay for all downlink packets.
- NumberUplinkPacket Count is the total amount of data sent in the uplink direction.
- The NumberDownlinkPackets is the number of packets received over the downlink channel.

In a network, jitter occurs when there is a fluctuation in the average delay of data packets due to issues like congestion, rerouting, or errors. Finding the mean delay deviation of all packets sent or received over a given period yields the

average jitter. (4) and (5) are the expressions for the same. The above calculation is only an approximation of the typical jitter and may not work in all situations. The real jitter experienced by a smartphone device in a 5G network might be affected by various factors such as network congestion, latency, and network conditions [52-54].

4. The average delay for camera and sensor applications

Calculating the average delay for camera and sensor applications in a 5G network is essential to evaluating network performance. Many factors can be accounted for in a calculation that estimates the average delay [8].

Estimating the average delay for camera and sensor applications in a 5G network requires the following formula:

$$AvgDelay = \left(\left(\frac{QueueLength * PacketSize}{LinkCapacity} \right) + ServiceTime \right) \quad (6)$$

Where,

- The QueueLength is the average number of packets in the transmission queue,
- The PacketSize is the size of each packet in bits,
- The LinkCapacity is the maximum data rate of the link in bits per second (bps), and
- The ServiceTime is the time required to transmit a single packet, including propagation delay and transmission time.

Typically, packet sizes for camera applications are larger because of the increased resolution and larger file sizes of photos and movies. Increased link capacity is required to meet the higher data rates associated with camera applications. In contrast, the packet size for sensor applications is smaller due to the smaller amount of data being broadcasted, and the connection capacity is lower since lower data rates are sufficient for the vast majority of sensor applications. (6) is the numerical expression for the average delay for camera and sensor applications. However, it is essential to note that the method only provides an estimate of the average delay and may not be appropriate in all situations. With a 5G network, additional factors such as network congestion, latency, and other network conditions can affect the real delay experienced by a camera or sensor equipment [52-58].

5. Average jitter for a camera or sensor

The average jitter for a camera or sensor in a 5G network can be calculated using the following formula [39-42].

$$AvgJitter = \frac{\sum \left(\left| \left(Time_n^a - Time_{(n-1)}^a - Time_{Expected}^{InterArrival} \right) \right| \right)}{(n-1)} \quad (7)$$

Where:

- $Time_n^a$ is the arrival time is the time at which packet "n" is received.
- $Time_{Expected}^{InterArrival}$ is the inter-arrival time is the time between two consecutive packet arrivals and it is proportional to the packet rate squared.

Jitter quantifies the randomness with which packets arrive at their destination. It can be brought on by anything that slows down the transmission of packets, including network congestion and changes in routing. With (7), we can determine how frequently packets arrive before or after their estimated inter-arrival time. Larger packet sizes and higher data rates can lead to increased variance in the transmission durations of packets, which can increase the jitter in a camera application. However, the jitter may be smaller in a sensor application because of the smaller packet sizes and lower data rates.

4. Materials and Methods

4.1 Experiment Set-up

Our aim in this investigation is to measure and analyze the impact of processing and decoding times on network performance across a variety of numerologies. We used Network Simulator 13 to create a test bed for a 5G network to achieve this. The flowchart of the investigation is shown in Fig. 1. The choice of the simulation tool is pivotal as it directly influences the accuracy and reliability of the simulation results. Among the various options available for simulating 5G networks are NS-3, OPNET Modeler, MATLAB with 5G toolkit, OMNeT++, QualNet, and NetSim 13.02. The researchers have selected NetSim 13.02 for this study because it adhered to 3GPP.XX specifications and its validation toolkit. Then, we designed and implemented the 5G Network Scenario, which involves defining the various components of the 5G network, such as base stations, user equipment (UE), core network elements, and the communication

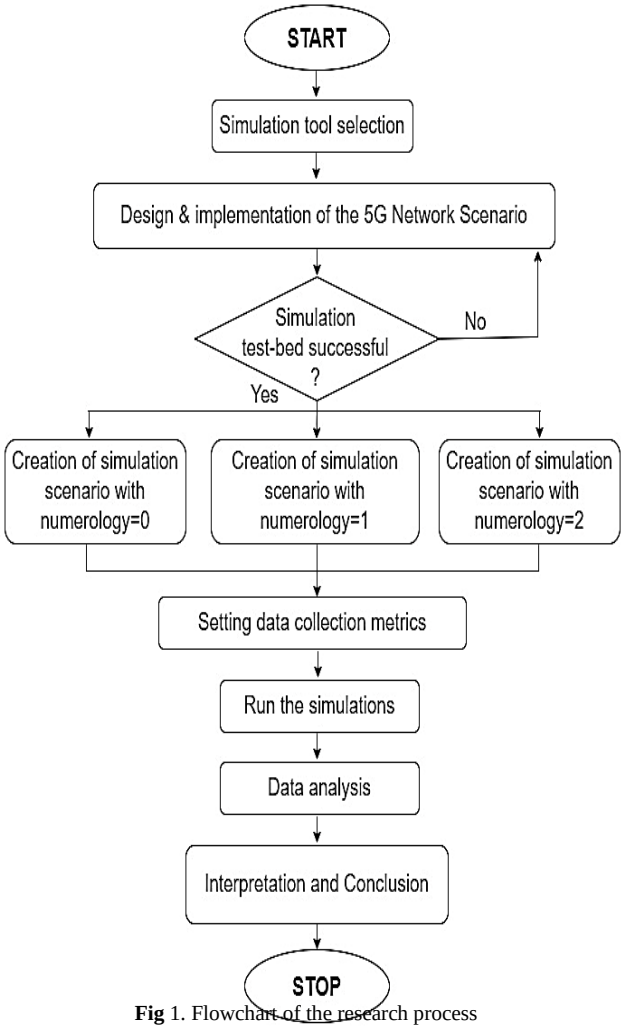

Fig 1. Flowchart of the research process

links between them. The simulation scenario considers different parameters and configurations, such as the number of base stations, their locations, mobility models of UEs, traffic patterns, and radio propagation models. The accuracy of the simulation results largely depends on how well the network scenario represents the real-world 5G deployment. After that, we created Simulation Scenario with numerology=1, 2, and 3: In 5G, numerology defines the subcarrier spacing and symbol duration used in the Orthogonal Frequency Division Multiplexing (OFDM) modulation scheme. Different numerology configurations have a significant impact on the data transmission rates and overall network performance. Therefore, this step involves creating multiple simulation scenarios, each with a different numerology setting (numerology=1, 2, and 3). These scenarios enable researchers to observe and analyze how varying subcarrier spacing affects the network's throughput, latency, and spectral efficiency. Then, we have defined the data collection metrics that will be used to measure the performance of the 5G network during simulations. These metrics include throughput, delay, latency, etc. By setting specific metrics, researchers can focus on gathering relevant data to address their research questions.

With the defined scenarios and data collection metrics, the actual simulations are executed. The simulation tool runs the network scenarios, and the performance data is collected based on the defined metrics. These simulations generate substantial data that will later be analyzed to draw meaningful conclusions. The collected data is then subjected to thorough analysis. We apply statistical and analytical techniques to interpret the data and identify patterns, trends, and relationships between different variables. This analysis helps in understanding the impact of subcarrier spacing on network performance and behavior. We interpret the simulation results based on the data analysis and statistical validation. We draw meaningful insights and conclusions about the effect of subcarrier spacing on the 5G network's performance. The interpretation aims to provide meaningful explanations for observed behaviours and performance variations.

Table 1 Equipment used in 5G test-bed

S.L No	Name
1	Smartphone
2	Sensor
3	CCTV camera
4	Database upload server
5	Database download server
6	Sensor server
7	Video server

This study's success lies in the careful design of the simulation scenario, accurate data collection, rigorous analysis, and meaningful interpretation of the results. Through such research endeavors, the understanding of 5G network behavior can be enhanced, leading to future more efficient and optimized network deployments. The numbers and types of equipment are carefully chosen for the test bed to accurately measure the impact of processing and decoding delays

on network performance across a variety of numerologies. Below is the list of equipment used:

Table 1 presents a comprehensive list of equipment employed in the investigation to evaluate the influence of processing and decoding times on network performance across different numerologies. Each equipment is assigned a unique number from 1 to 7, along with their respective names, which are as follows: -

- Smart Phone: This device likely serves as a mobile testing tool, facilitating the simulation of user interactions within the 5G network environment.
- Sensor: Sensors play a crucial role in data collection and transmission, enabling real-time assessment of data transfer and processing within the network.
- CCTV Camera: This equipment is specifically utilized to monitor and analyze video data transmission over the 5G network.
- Database Upload Server: This server is responsible for uploading data to the network's database and aiding in measuring the impact of processing delays during data uploads.
- Database Download Server: This server is utilized to download data from the network's database, facilitating the analysis of decoding times during data retrieval.
- Sensor Server: This server is dedicated to handling and managing various sensors in the network, allowing for controlled testing of sensor data.
- Video Server: The video server plays a vital role in assessing video streaming and has impact on network performance, particularly in terms of processing and decoding delays.

Table 2 presents details about the smartphone device type, consisting of 25 units with a fixed mobility status. It provides an overview of various transport layer properties, such as utilizing the "New Reno" congestion control algorithm, a maximum of 5 SYN retries, and an un-delayed acknowledgement type. The maximum segment size is 1460 bytes, and the time-wait-timer is set to 120 seconds.

Communication within the device is facilitated through the UDP protocol. The interface properties are described, including the 3GPP series noted as 38, a transmitter power of 23 dBm, and the protocol specified as LTE NR. The Smartphone is equipped with 4 transmitter antennas and 2 receive antennas. The application properties indicate the use of unicast as the application method, with FTP (File Transfer rotocol) as the designated application type, and the Quality of Service (QoS) set to Best Effort. The device maintains a constant file distribution strategy, with an upload file size of 1.5 Mb and a download file size of 25 Mb. Additionally, the inter-arrival time for data is set to 200 seconds. The second type of equipment used in the 5G network is CCTV cameras and sensors. The CCTV camera and the sensors can be used to collect various types of environmental data for wireless sensor networks or Internet of Things networks. The sensors normally transmit huge amounts of data. The details of various 5G parameters used for the sensors and CCTV camera are mentioned in Table 3 and Table 4, respectively.

Table 2.5G parameters used for sensors

Device Type		Sensor
Count		6
Mobility		no
Transport layer Properties	Congestion control algorithm	New Reno
	Max SYN retries	5
	Acknowledge type	Un-delayed
	Maximum segment size (Byte)	1460
	Time-wait-timer (Seconds)	120
	Protocol	UDP
Interface Properties	3GPP series	38
	Transmitter Power (dBm)	23
	Protocol	LTE NR
	Transmitter Antenna count	4
	Receive Antenna count	2
Application Properties	Application method	Unicast
	Application Type	FTP
	QoS	Best Effort
	File Distribution	Constant
	File Size	55 Mb
	Inter arrival time (in Micro Sec.)	250

Table 3 provides a detailed overview of a specific device type known as "Sensor." The investigation includes a total of four sensors, each fixed in position with no mobility. The properties of these sensors are thoroughly presented. For the transport layer, the sensors utilize the "New Reno" congestion control algorithm, accommodating a maximum of 5

SYN retries, and implement an un-delayed acknowledgement type. The maximum segment size is set to 1460 bytes, and a time-wait-timer of 120 seconds is used. The sensors operate with the UDP (User Datagram Protocol) for com nication. In terms of interface properties, they belong to the 3GPP series 38 and function with a transmitter power of 23 dBm. The sensors utilize the LTE NR (New Radio) protocol and are equipped with four transmitter antennas and two receiver antennas. As for application properties, data transmission is performed using the unicast method, and the application type specified is FTP (File Transfer Protocol). The sensors are configured with a "Best Effort" Quality of Service (QoS) and constantly distribute files with a size of 55 megabytes. The inter-arrival time for data is measured in microseconds, and there is an interval of 250 microseconds between successive data arrivals.

Table 3 5G parameters used for the Smartphone

Device Type		Smartphone
Count		25
Mobility		No
Transport Layer Properties	Congestion control algorithm	New Reno
	Max SYN retries	5
	Acknowledge type	Un-delayed
	Maximum segment size (Byte)	1460
	Time-wait-timer (Seconds)	120
	Protocol	UDP
Interface Properties	3GPP series	38
	Transmitter Power (dBm)	23
	Protocol	LTE NR
	Transmitter antenna count	4
	Receive antenna count	2
Application Properties	Application method	Unicast
	Application type	FTP
	QoS	Best Effort
	File distribution	Constant
	Upload file size	1.5 Mb
	Download file size	25 Mb
	Inter arrival time (in Sec.)	200

Table 4 presents comprehensive information about the "CCTV Camera" device category, which includes a total of 5 units and is designed to be stationary, meaning it does not have mobility. The transport layer properties specify the utilization of the "New Reno" congestion control algorithm with a maximum of 5 SYN retries and immediate acknowl edgements. Data transmission is limited to a maximum segment size of 1460 bytes, and a time-wait-timer of 120 seconds is configured. The protocol used for communication is UDP (User Datagram Protocol). Concerning interface properties, the device adheres to the 3GPP series 38 standards and operates on the "LTE NR" protocol. It is equipped with 4 transmitter antennas and 2 receiver antennas, enhancing its communication capabilities. The camera device maintains a constant file distribution strategy, where each file has a size of 500 bytes. Additionally, the inter-arrival time for data is set to 800 microseconds, ensuring controlled data flow in the network.

Table 4 5G parameters used for the CCTV camera

Device Type		Camera
Count		5
Mobility		no
Transport layer Properties	Congestion control algo	New Reno
	Max SYN retries	5
	Acknowledge type	Undelayed
	Maximum segment size (Byte)	1460
	Time-wait-timer (Seconds)	120
	Protocol	UDP
Interface Properties	3GPP series	38
	Transmitter Power (dBm)	23
	Protocol	LTE NR
	Transmitter Antenna count	4
	Receive Antenna count	2
Application Properties	Application method	unicast
	Application Type	CUSTOM
	QoS	Best Effort
	File Distribution	Constant
	File Size	500 MB
	Interarrival time (in micro)	800

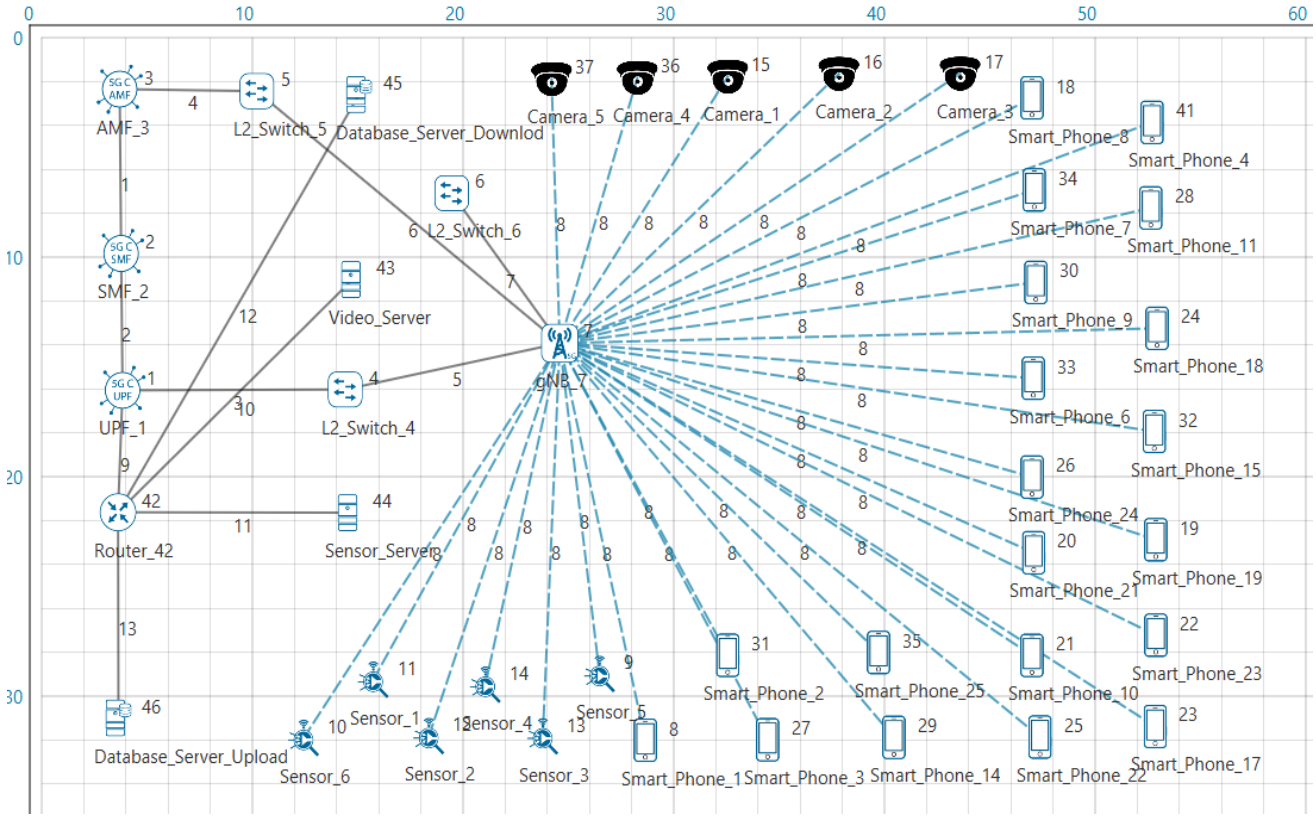

Fig 2. 5G Simulation Test-bed setup

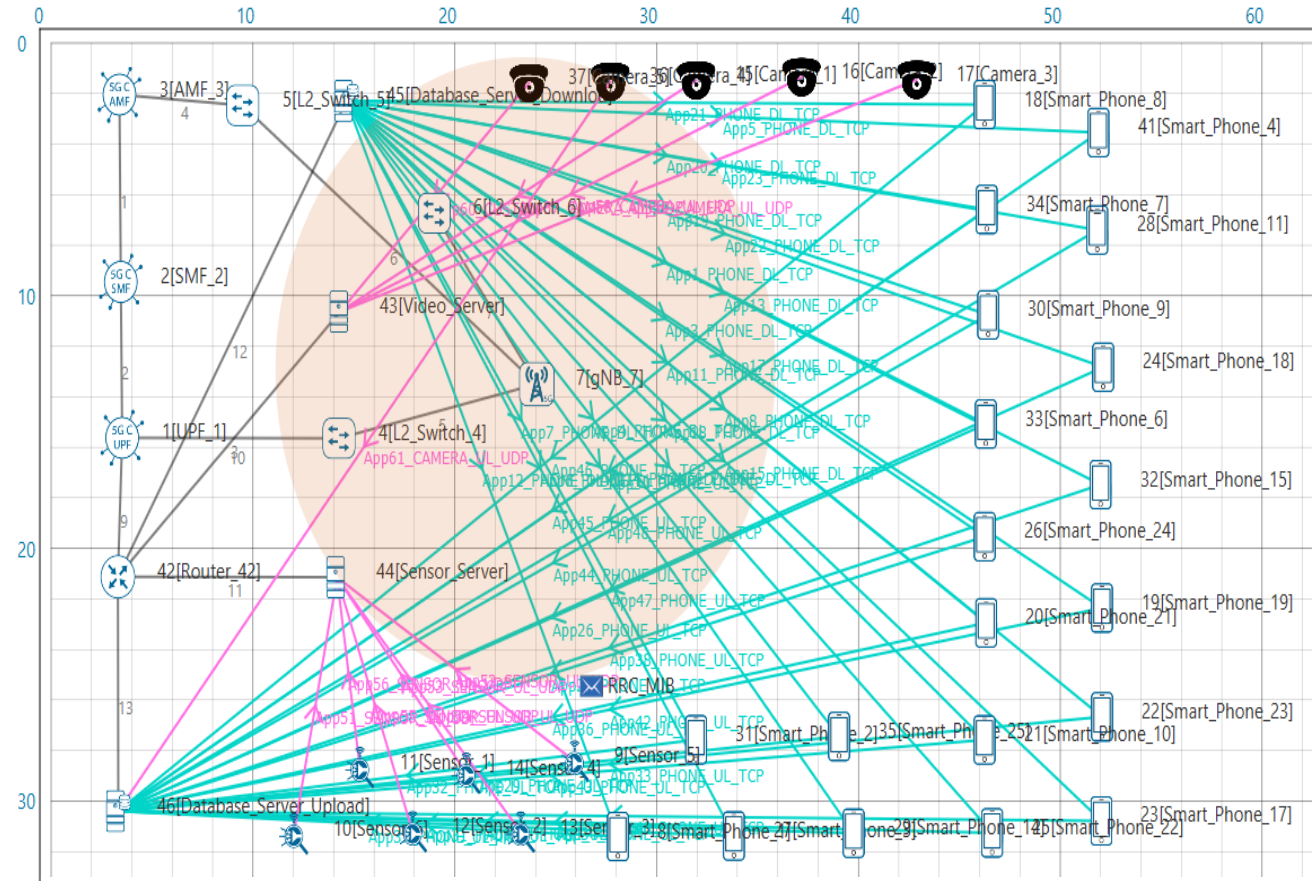

Fig 3. Test-bed with control signal transmission

Fig. 2 shows the snapshot of the simulation test-bed of the 5G network involving various types of equipment. The figure also shows the placement, proximity, and connections of equipment with respect to each other. To make the figure cognizable we have clustered each type of equipment. All the smartphones, CCTV and cameras are connected to gNB. Fig. 3 shows a 5G Simulation test bed with control signal transmission. For the 5G simulation, control signal transmission plays a significant role in managing and coordinating various aspects of the network. Control signals serve as crucial messages exchanged between different network elements to control and optimize overall network performance. These signals are responsible for handling essential tasks such as network access, resource allocation, handovers, and scheduling of user equipment (UE) connections. Fig. 3 shows control signal transmission works in the 5G simulation:

- Resource Allocation: Control signals efficiently allocate network resources, including frequency bands, time slots, and other communication resources, based on the specific requirements of different users and services.
- Initial Access: When a new device or user equipment (UE) seeks to join the 5G network, an initial connection must be established. Control signals facilitate this process, enabling the UE to synchronize with the network and establish a communication link.
- Mobility Management: 5G networks are designed to handle various mobility scenarios. Control signals are instrumental in managing mobility by facilitating seamless handovers between different base stations as users move within the network coverage area.
- Connection Setup and Release: Control signals handle the setting up and releasing of connections between UEs and the network. Whether a user wants to initiate or end a data session, control signals are responsible for managing the connection establishment and release procedures.
- Quality of Service (QoS) Management: 5G networks support various services with diverse QoS requirements. Control signals enforce QoS parameters, ensuring each service receives appropriate network resources and priority levels.
- Beamforming and MIMO: In 5G networks, advanced antenna techniques like beamforming and Multiple-Input Multiple-Output (MIMO) enhance data rates and coverage. Control signals are vital in steering the beams and optimizing MIMO configurations.
- Network Optimization: Control signals can carry information about network performance and status. Network management systems utilize this information to optimize various parameters, enhancing overall network efficiency.
- Scheduling: In a multi-user environment, control signals are instrumental in scheduling transmission slots for different UEs. This scheduling process considers factors such as quality, priority, and traffic demands.

Accurate modelling and simulation of control signals are essential in a 5G simulation, as they help researchers and network engineers analyze and optimize the network's behaviour under various scenarios and conditions. This aids in designing and deploying efficient and reliable 5G networks that can effectively meet the demands of modern communication services and applications.

4.2 Adaptive Algorithm for Dynamic SCS Adjustment

We have developed and tested an adaptive algorithm using Q-learning [59]. The algorithm was designed to modify SCS settings in response to real-time network characteristics, including jitter, throughput, and delay. The method is designed to enhance data transmission efficiency for various applications on devices such as cameras, sensors, and smartphones. The algorithm is shown in Table 5.

Table 5 Algorithm for dynamic SCS adjustment

1. State Space:
• Each state is represented by a combination of jitter, throughput, and delay levels (3 jitter levels × 3 throughput levels × 3 delay levels = 27 states). E.G., States for the camera (Low, Medium, High). Jitter (ms): Low < 200, Medium 200-300, High > 300 Delay (ms): Low < 800, Medium 800-1600, High > 1600 Throughput (Mbps): Low < 20000, Medium 20000-60000, High > 60000
2. Action Space:

Actions correspond to selecting an SCS value: {15 kHz, 30 kHz, 60 kHz}.

3. Reward Function:

- The reward function is designed to encourage actions that improve network performance and meet application requirements. We have defined rewards based on the following criteria:
  - Positive reward (+10) for reduced jitter, increased throughput, and decreased delay.
  - Penalties (-10) for performance degradation.
  - No reward for no change in performance.

4. Dynamic SCS Adjustment using Q-Learning Algorithm:

```
Algorithm Q-Learning
Input: alpha, gamma, epsilon, num_states, num_actions
Initialize Q[state, action] to 0 for all states and actions
    Define num_episodes = 1000
    Define max_steps = 100
    for episode from 0 to num_episodes - 1 do
        current_state = random_state()
        for step from 0 to max_steps - 1 do
            if random_number() < epsilon then
                action = random_action()
            else
                action = argmax(Q[current_state, :])
            end if
(reward, next_state) = get_reward_next_state(current_state, action)
Q(current_state, action) ← Q(current_state, action)
+α[r + γmax_a Q(next_state, next_action)
−Q((current_state, current_action))]
            current_state = next_state
        end for
    end for
End Algorithm
```

The state space refers to the various network states, including jitter, throughput, and latency. Each state is a composite of these three factors at various levels. For the camera and sensor, the Jitter, measured in milliseconds (ms), is Low when below 200 ms, Medium between 200 and 300 ms, and High over 300 ms. Low delay, measured in milliseconds, is less than 800 ms, Medium is 800–1600 ms, and High is 1600+ ms. Throughput, measured in (Mbps, is Low when below 20000 Mbps, Medium between 20000 and 60000, and High above 60000. Similarly, for smartphones, Low jitter is less than 40 ms, Medium is 40–80 ms, and High is 80+ Microseconds. Delay, measured in microseconds, is Low if under 20,000, Medium if 20,000–60,000, and High if over 60,000. Throughput, defined in megabits per second (Mbps), is Low below 125 Mbps, Medium between 125 and 250 Mbps, and High over 250 Mbps.

The reward function guides the learning process by providing feedback on actions. It encourages actions that improve network performance and penalizes actions that degrade performance.

- Positive Reward (+10):
  - Given for actions that result in reduced jitter, increased throughput, and decreased delay.
- Penalty (-10):
  - Given for actions that lead to increased jitter, decreased throughput, and increased delay.
- No Reward (0):
  - Given for actions that result in no change in performance.

The learning rate, denoted by alpha, determines how much new information overrides the old information. The discount factor, represented by gamma, determines the importance of future rewards. The exploration rate, indicated by epsilon, determines the probability of exploring new actions versus exploiting known ones. In this case, the total number of states is 27, and the total number of actions is 3. Specifically, the learning rate (alpha) is set to 0.1, the discount factor (gamma) is 0.9, and the exploration rate (epsilon) is 0.1.

The Q-learning technique involves iteratively enhancing the policy for selecting SCS values according to network conditions. At the beginning of each episode, the algorithm sets the current state to a randomly selected state. During each episode, the algorithm determines whether to explore or exploit for a specific number of steps. When a randomly generated number is smaller than the exploration rate

(epsilon), a random action is chosen (exploration); otherwise, the action with the highest Q-value for the current state is selected (exploitation). Once an action is chosen, the algorithm takes note of the reward that follows and the subsequent state. The Q-value for the current state-action pair is updated using the following formula:

$$\mathbf{Q}(\mathbf{s},\ \mathbf{a}) \leftarrow \mathbf{Q}(\mathbf{s},\ \mathbf{a}) + \boldsymbol{\alpha}[r + \gamma \mathbf{max}_{\mathbf{a}'}\mathbf{Q}(\mathbf{s}', \mathbf{a}') - \mathbf{Q}(\mathbf{s}, \mathbf{a})] \quad (8)$$

where,

- Q(s,a): The current Q-value for state s and action a.
- **α** is the learning rate, which determines how much new information overrides the old information.
- **r** is the reward received after taking action a in state s.
- **γ** is the discount factor, which determines the importance of future rewards.
- $\mathbf{max}_{\mathbf{a}'}\mathbf{Q}(\mathbf{s}', \mathbf{a}')$ is the maximum Q-value for the next state s′ over all possible actions a′.
- **s** is the current state.
- **a** is the current action.
- **s′** is the next state resulting from taking action a′

This update considers both the immediate benefit and the reduced maximum future payout. Ultimately, the present condition is modified to the subsequent condition, and the procedure continues to occur repeatedly. The iterative technique enables the programme to get the optimal policy for dynamically enhancing network performance by modifying SCS levels.

5. Results and Discussions

5.1 Performance evaluations of devices in various SCS values

A detailed analysis of the average throughput values for both the uplink and downlink of a smartphone at various numerology values is presented in Fig. 4. Numerology represents the subcarrier spacing in the communication system, and the analysis aims to understand the impact of different subcarrier spacing on the Smartphone's throughput performance. The analysis reveals that the Smartphone's throughput performance varies notably between the uplink and

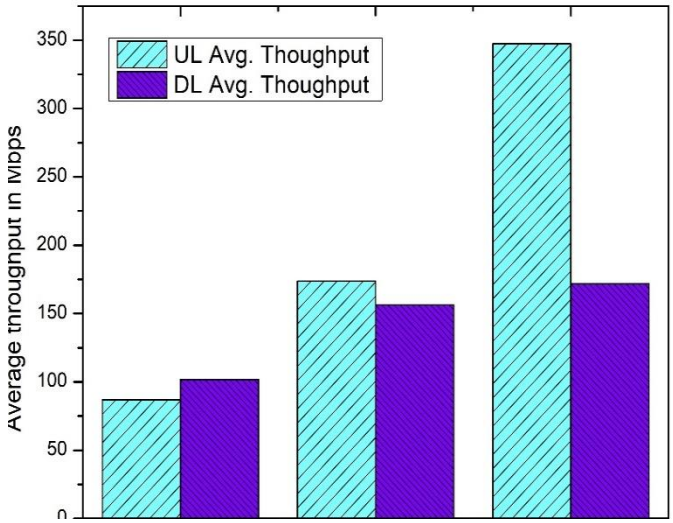

Fig 4. 5G network average throughput for uplink and downlink of smartphone

downlink directions at different numerology settings. At numerology = 3, the uplink exhibits significantly higher throughput (347.302 Mbps) than the downlink (76.87 Mbps). At numerology = 2, both uplink and downlink show lower throughput values, with a less pronounced difference between them. Interestingly, at numerology = 1, the downlink achieves higher throughput (114.47 Mbps) than the uplink (86.920 Mbps).

These findings indicate that the choice of numerology setting can considerably impact the Smartphone's data transmission performance in different directions. Understanding this throughput variation is crucial, especially for applications with asymmetric data requirements, where data transfer

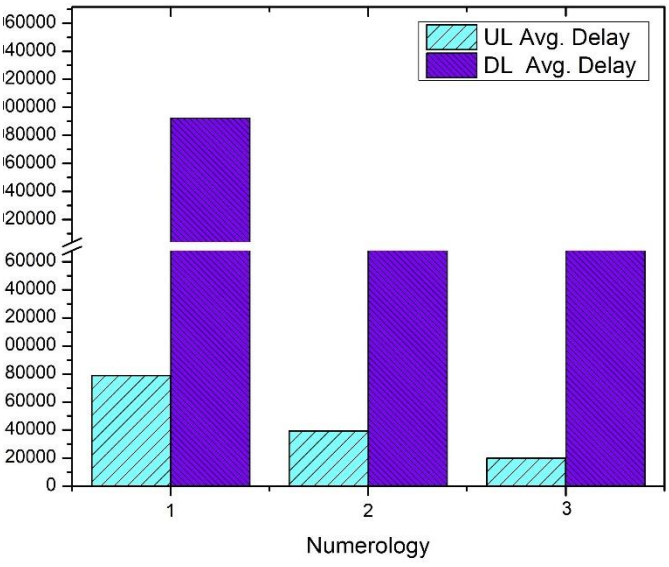

Fig 5. 5G network average delay for uplink and downlink of Smartphone

is more significant in one direction. Additionally, this analysis helps optimize data transmission for specific application needs, considering the trade-offs between higher throughput and subcarrier spacing settings based on the performance requirements and priorities of the application. Fig. 5 presents a detailed analysis of the average delay values for the uplink and downlink of a smartphone at various numerology values. Numerology represents the subcarrier spacing in the communication system, and the goal of the analysis is to explore how the Smartphone's delay performance is affected by different subcarrier spacing settings. The findings indicate that the Smartphone demonstrates consistent and balanced delay performance across all numerology values in uplink and downlink directions. At numerology = 3, 2, and 1, the average delay remains constant for uplink and downlink, indicating a symmetrical delay experience suitable for bidirectional communication. This balanced delay performance is advantageous for applications requiring bidirectional data transmissions, such as real-time video calls or online gaming. It ensures that delays experienced in both directions are similar, enhancing the overall user experience. However, it is crucial to consider specific application requirements when choosing the appropriate numerology setting, as there are trade-offs between lower delays and data throughput. Lower numerology values may be preferable for latency-sensitive applications to achieve reduced delays. In comparison, higher numerology values may be more suitable for data-intensive applications prioritizing higher data throughput. The analysis offers valuable insights into the Smartphone's delay performance, guiding informed decisions regarding bidirectional communication needs and performance considerations at different numerology values.

Fig. 6 presents a detailed analysis of the average jitter values for the uplink and downlink of a smartphone at various numerology values. Numerology represents the subcarrier spacing in the communication system, and the analysis aims to understand how the Smartphone's jitter performance varies with different subcarrier spacing settings. The analysis reveals that the Smartphone's jitter performance differs between the uplink and downlink directions at different numerology settings. At numerology = 3, the downlink experiences a slightly higher jitter than the uplink. In contrast, at numerology = 2, both uplink and downlink exhibit symmetrical jitter values. At numerology = 1, there are minor variations in jitter between the two directions. Comprehending this jitter behaviour is crucial for applications requiring bidirectional communication and prioritizing consistent data transmission.

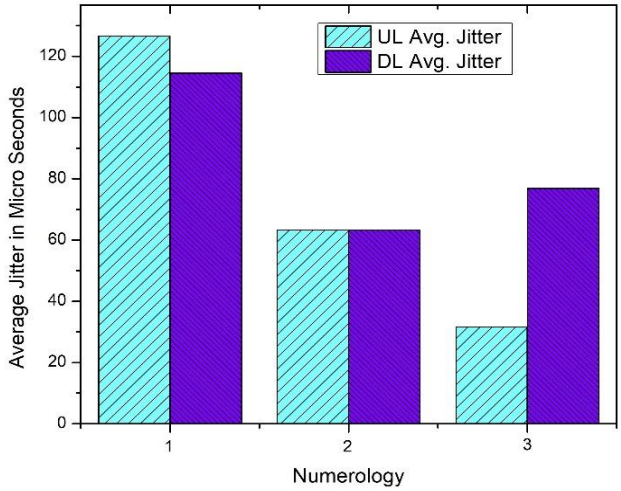

Fig 6. 5G network average jitter for uplink and downlink of Smartphone

The symmetrical jitter values observed at numerology = 2 might be preferred for such applications. However, for applications sensitive to jitter, a careful balance between lower jitter values and data throughput is necessary when selecting the optimal numerology setting based on specific requirements.

The presented Fig. 7 comprehensively compares average delay values for both a camera and a sensor at various numerology settings. Numerology represents the subcarrier spacing in a communication system, and the analysis aims to explore the delay performance of the devices under different subcarrier spacing conditions. At numerology = 3, the camera exhibits a significantly lower average delay of 477.03 ms than the sensor's 778.63 ms. This implies that the camera's data transmission is more responsive, experiencing less delay at this specific subcarrier spacing setting. As the numerology reduces to 1, the camera and sensor encounter an increase in average delay. However, even at numerology = 2, the camera continues outperforming the sensor with a delay of 931.11 ms compared to the sensor's 1533.30 ms. Similarly, at Numerology = 1, the camera maintains its performance advantage, displaying an average delay of 1839.07 ms, while the sensor's delay increases to 2283.62 ms. Consequently, the camera outperforms the sensor across all numerology values concerning the average delay. This suggests

that the camera is more responsive and exhibits quicker data transmission capabilities than the sensor, making it more suitable for applications that demand low delay and high responsiveness. Moreover, it is important to note that both devices experience an increase in average delay as the numerology decreases. This trend is expected as larger subcarrier

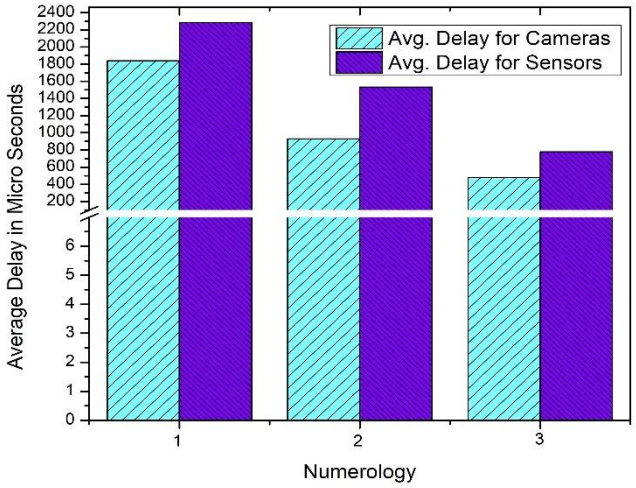

Fig 7. 5G network average delays for camera and sensors

spacing allows for greater data transmission capacity, reducing delays. Conversely, smaller subcarrier spacing accommodates higher data transfer rates but may result in increased delays due to greater data processing requirements. The selection between the camera and sensor should be thoughtfully considered based on the specific application requirements. For real-time applications demanding low delay and high responsiveness, the camera proves to be the optimal choice. However, the sensor may be more suitable in data-intensive applications prioritizing data throughput over delay, especially at smaller numerology values. Overall, this analysis facilitates a deeper understanding of the delay performance of the devices and supports informed decisions based on the application's performance needs, considering the trade-offs between delay, data throughput, and responsiveness.

Fig. 8 illustrates 5G network performance for CCTV cameras and sensor devices. The graph depicts the effect of numerologies/subcarrier spacing on the average jitter of CCTV cameras and sensors connected to a 5G network. Numerologies have a positive effect on the CCTV cameras' ability to reduce average jitter. With numerology equivalent to zero, the average jitter for sensors is exceptionally high. Nonetheless, when numerology is set to 2 or subcarrier spacing is set to 30 kilohertz, the average disturbance is drastically reduced, whereas it increases slightly when numerology is set to 3. Fig. 8 highlights that the camera's average jitter fluctuates across different numerology values, with the lowest jitter observed at numerology =3 and the highest at numerology =1. This suggests that the camera experiences more stable data transmission at numerology =3, while at numerology =1, the data transmission encounters higher jitter. In contrast, the sensor's average jitter remains consistently low across all numerology values, indicating highly stable data transmission regardless of the numerology setting. The analysis of the figure points out that the sensor consistently outperforms the camera in terms of jitter. Even at its highest jitter value (0.37 ms), the sensor's performance remains significantly better than the camera's best-performing value at numerology =3 (151.91 ms). This observation highlights the sensor's superior stability and reliability in data transmission compared to the camera, which exhibits more variation in delay under different numerology conditions. In contrast to the camera's variability, the figure highlights that the sensor maintains its low jitter values consistently across all numerology values. This consistency in the sensor's performance indicates its robustness and ability to deliver stable data transmission regardless of the numerology setting. The sensor's performance consistency is advantageous in critical applications where reliable and low-latency data delivery is essential.

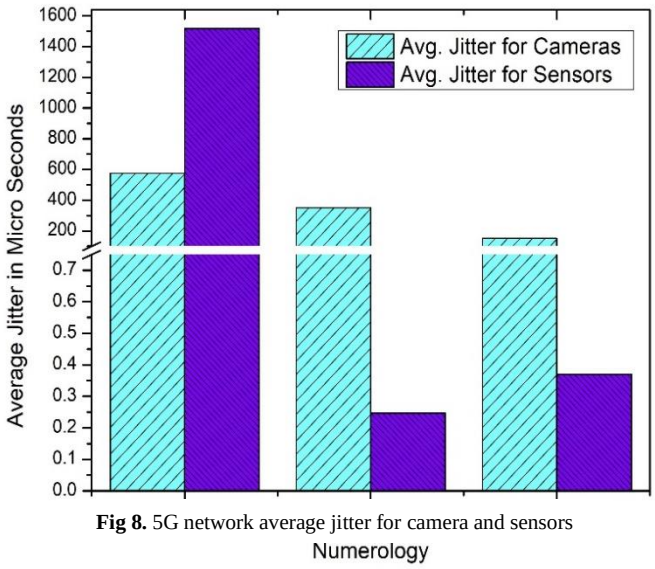

Fig 8. 5G network average jitter for camera and sensors

The figure emphasizes that the choice of numerology value should be based on the specific requirements and priorities of the application. If low jitter is a critical requirement, the stability exhibited by the sensor across all numerology values might be preferred. On the other hand, if high data throughput is the priority, the camera's relatively lower jitter at higher numerology values might be acceptable in certain scenarios, depending on the specific characteristics of the application. Ultimately, the selection of the optimal numerology should be based on a comprehensive understanding of the specific application's needs and the trade-offs between data throughput and jitter stability. Each numerology offers distinct advantages, and the choice of numerology value should align with the application's performance requirements and priorities. An informed decision can lead to an effective and reliable data transmission system that meets the specific demands of the intended use case.

The parameters used in the study [60] include a 3GPP channel model and the NewReno congestion control algorithm, with a segment size of 1400 bytes for Video, smartphone upload and download. While these parameters remain consistent with this article's simulation environment setup, some aspects differ. Specifically, a segment size of 500 bytes for the sensor. Also, the authors of the article [60] considered TCP connections for upload and downlink connection in Smartphonethe smartphones. The channel condition is also set to Line-Of-Sight, with a channel bandwidth of 100 MHz and a central frequency of 28 GHz. The scenario is described as Urban (UMa), and no shadowing is applied. An adaptive Modulation Coding Scheme is also used, with control/data encoding latency set to 2 slots, and the radio scheduler operates on a Round-Robin basis.

Table 6 Performance Evaluation [60]

	SCS-15	SCS-30	SCS-60
Smartphone Upload	18 Mbits/sec	65 Mbits/sec	110 Mbits/sec
smartphone Download	23 Mbits/sec	90 Mbits/sec	150 Mbits/sec
Sensor delay	1.75 ms	1.7 ms	0.3 ms
Video delay	1.5 ms	0.8 ms	1ms

The simulation results in Table 6 of [60] and this article are comparable. Notably, the results for smartphones across different SCS values show better performance in our study, which can be attributed to using UDP connections for smartphones. Additionally, it is essential to highlight that the study in [60] did not consider jitter in its performance evaluation.

5.2 Testing of adaptive SCS adjustment algorithm

The proposed adaptive SCS adjustment algorithm is based on the Q-learning algorithm, which is a type of reinforcement machine-learning algorithm, as mentioned in section 4.2. The algorithms take real-time network conditions and application requirements as input to produce the optimal SCS value recommended for that application. Fig 9 shows how a decision is made for optimal SCS configuration using a Q learning agent.

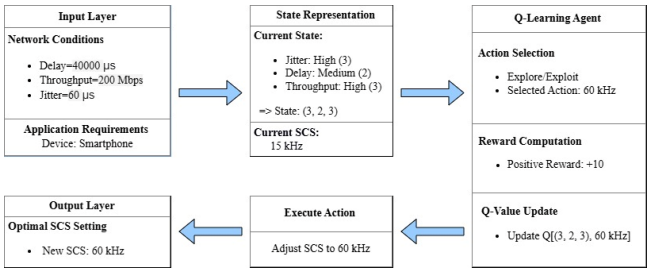

Fig. 9 Output produced by the proposed adaptive SCS adjustment algorithm

The input layer in Fig. 9 accepts information on the network's real-time condition and application requirements. In this case, the input includes values such as a delay of 40 milliseconds, a jitter of 60 µs, and a throughput of 200 Mbps for an instance of network condition. A composite of the following levels characterizes the current state: significant variation in data transmission delay (3 for high), moderate latency (2 for medium), and substantial data transfer rate (3 for high), resulting in the state (3, 2, 3). The Q-learning agent subsequently determines the SCS value, opting for 60 kHz in this instance, using an exploration/exploitation technique. The reward is calculated based on the enhancement in performance, and the Q-value table is subsequently updated. The chosen operation, with a frequency of 60 kHz, is performed to adjust the SCS. Finally, the most favourable SCS configuration, which, in this particular case, is set at 60 kHz, is produced at the output. This block diagram (Fig. 9) illustrates the sequential transfer of information from the initial condi-

tions to the Q-learning agent, which then determines the optimal SCS setting for the output. This figure demonstrates the system's ability to adapt and enhance network performance.

The article [11] introduces an adaptive system architecture that adjusts transmission configurations to meet strict reliability criteria. The adaptive numerology selection algorithm dynamically adjusts transmission parameters like subcarrier spacing and symbol duration based on estimated channel factors like SNR, delay spread, and Doppler spread. Here, we have provided a comparison between the proposed algorithm in this article and the algorithm proposed in [11], which are as follows:

Table 7 Performance Comparison

Parameter	Proposed Algorithm	[11]
Algorithm Basis**:**	Utilizes a Q-learning algorithm that prioritizes real-time learning and adaptation according to network conditions.	Utilizes an approach that involves modifying the number of pilots and control plane overhead, in addition to the use of SCS.
Parameters Considered**:**	Examines the factors of jitter, throughput, and latency.	Emphasizes the concentration of pilots and the additional computational overhead of the control plane to enhance SCS adjustments.
Adaptation Mechanism**:**	Utilizes a q-learning reinforcement learning methodology in which the algorithm progressively enhances its performance through rewards.	Applies predetermined mechanisms that rely on pilot density and CP adjustments to ensure consistent performance in different conditions.
Target Outcomes**:**	Seeks to improve the overall efficiency of data transmission for different applications.	Aims to meet QoS standards and achieve a low Bit Error Rate (BER), particularly in high-speed situations.

6. Conclusion

Our analysis of average throughput, delay and jitter values across smartphones, cameras, and sensors at varying numerology (SCS) values offers valuable insights into their respective data transmission performances. Higher numerology values, such as numerology = 3, correlate with increased average throughput in smartphones, indicating that larger subcarrier spacing facilitates more efficient data transmission. Conversely, lower numerology values, like numerology = 0, lead to decreased throughput, likely due to higher data processing requirements. Furthermore, smartphones exhibit relatively low and symmetrical jitter at numerology = 3 and 2, making them well-suited for bidirectional communication. Contrarily, the camera consistently demonstrates lower delay values, showcasing its capability for low-latency data transmission. At the same time, the sensor outperforms the camera in terms of jitter, highlighting its stability and reliability in data delivery. Configuring smartphones with higher numerology values is advisable for applications prioritizing high data throughput. Conversely, opting for the sensor over the camera may be preferred in scenarios where stability and low jitter are crucial. Also, the proposed adaptive algorithm automatically presents optimal SCS configurations based on real-time network conditions and application needs. The algorithm employs simulation and machine learning techniques for enhancing network performance under different circumstances.

Future research could explore additional factors impacting data transmission performance, such as channel conditions, antenna configurations, and network congestion. Investigating the interaction between different devices in a multi-user environment could yield valuable insights.

References

[1] S. Li, T. Xiang, D. Huang, L. Han, Q. Wu, and D. Kong, "An Efficient Random Access Reception Algorithm for ToA Estimation in NB-IoT", *Electronics*, vol. 12, no. 12, p. 2636, 2023. DOI: 10.3390/electronics12122636

[2] R. Poorzare and O. P. Waldhorst, "Toward the Implementation of MPTCP Over mmWave 5G and Beyond: Analysis, Challenges, and Solutions", *IEEE Access*, vol. 11, pp. 19534-19566, 2023. doi: 10.1109/access.2023.3248953

[3] P. Wang, Y. Li, Y. Lin, M. Shirvanimoghaddam, O. S. Park, G. Park, and B. Vucetic, "Analysis of Rateless Multiple Access Scheme with Maximum Likelihood Decoding in an AWGN Channel", *IEEE Transactions on Wireless Communications*, 2023. doi: 10.1109/twc.2022.3232781

[4] F. Boccardi, R. W. Heath, A. Lozano, T. Marzetta, and P. Popovski, "Five disruptive technology directions for 5G", *IEEE Communications Magazine*, vol. 52, no. 2, pp. 74-80, 2014. doi: 10.1109/mcom.2014.6736746

[5] Y. Liu, Z. Qin, M. Elkashlan, Z. Ding, A. Nallanathan, and L. Hanzo, "Non-Orthogonal Multiple Access for 5G and Beyond", *IEEE Communications Magazine*, vol. 55, no. 2, pp. 210-217, 2017. doi: 10.1109/jproc.2017.2768666

[6] E. Dahlman, S. Parkvall, and J. Skold, "5G NR: The next generation wireless access technology", Academic Press, 2020. doi: 10.1016/b978-0-12-814323-0.00005-3

[7] E. Dahlman, S. Parkvall, and J. Skold, "5G NR: The next generation wireless access technology", *Academic Press*, 2018. doi: 10.1016/b978-0-12-814323-0.00005-3

[8] M. Abd-Elnaby, G. G. Sedhom, E. S. M. El-Rabaie, and M. El-wekeil, "NOMA for 5G and beyond: literature review and novel trends", *Wireless Networks*, vol. 29, no. 4, pp. 1629-1653, 2023. doi: 10.1007/s11276-022-03175-7

[9] M. Raftopoulou and R. Litjens, "Optimization of numerology and packet scheduling in 5G networks: To slice or not to slice?," *2021 IEEE 93rd Vehicular Technology Conference (VTC2021-Spring)*, 2021, pp. 1-5. doi: 10.1109/VTC2021-Spring51267.2021.9448814

[10] A. Yazar and H. Arslan, "Reliability enhancement in multi-numerology-based 5G new radio using INI-aware scheduling," *EURASIP Journal on Wireless Communications and Networking*, vol. 2019, no. 1, pp. 1-14, 2019. doi: 10.1186/s13638-019-1435-z

[11] Soni, Tapisha, Ali, A. R., Ganesan, K., & Schellmann, M,"Adaptive numerology—A solution to address the demanding QoS in 5G-V2X", *IEEE Wireless Communications and Networking Conference (WCNC)*. IEEE, 2018. doi: 10.1109/WCNC.2018.8377205

[12] Correia, N., Al-Tam, F., & Rodriguez, J. "Optimization of mixed numerology profiles for 5G wireless communication scenarios.", *Sensors*, 21(4), 1494.2021 doi: 10.3390/s21041494

[13] X. Gao, L. Dai, S. Han, I. Chih-Lin, & R. Heath, "Energy-efficient hybrid analog and digital precoding for mmwave mimo systems with large antenna arrays", *IEEE Journal on Selected Areas in Communications*, vol. 34, no. 4, p. 998-1009, 2016. doi: 10.1109/jsac.2016.2549418

[14] T. Kebede, Y. Wondie, J. Steinbrunn, H. Belay, & K. Kornegay, "Precoding and beamforming techniques in mmwave-massive mimo: performance assessment", *IEEE Access*, vol. 10, p. 16365-16387, 2022. doi: 10.1109/access.2022.3149301

[15] C. Fischione, D. Koutsonikolas, S. Rangan, J. Widmer, X. Zhang, & A. Zhou, "Guest editorial millimeter-wave networking", *IEEE Journal on Selected Areas in Communications*, vol. 37, no. 12, p. 2649-2652, 2019. doi: 10.1109/jsac.2019.2947996

[16] J. Yang, S. Jin, Y. Han, M. Matthaiou, & Y. Zhu, "3-d position and velocity estimation in 5g mmwave cran with lens antenna arrays", *IEEE xplore*, 2019. doi: 10.1109/vtcfall.2019.8891333

[17] A. Shallah, F. Zubir, M. Rahim, H. Majid, U. Sheikh, N. Muradet al., "Recent developments of butler matrix from components design evolution to system integration for 5g beamforming applications: a survey", *IEEE Access*, vol. 10, p. 88434-88456, 2022. doi: 10.1109/access.2022.3199739

[18] J. Lota, S. Sun, T. Rappaport, & A. Demosthenous, "5g uniform linear arrays with beamforming and spatial multiplexing at 28, 37, 64, and 71 ghz for outdoor urban communication: a two-level approach", *IEEE Transactions on Vehicular Technology*, vol. 66, no. 11, p. 9972-9985, 2017. doi: 10.1109/tvt.2017.2741260

[19] L. Mendes, J. Vaz, F. Passos, N. Lourenço, & R. Martins, "In-depth design space exploration of 26.5-to-29.5-ghz 65-nm cmos low-noise amplifiers for low-footprint-and-power 5g communications using one-and- two -step design optimization", *IEEE Access*, vol. 9, p. 70353-70368, 2021. doi: 10.1109/access.2021.3078240

[20] Z. Yuan, T. Azzino, H. Yu, Y. Lyu, H. Pei, A. Boldiniet al., "Network-aware 5g edge computing for object detection: augmenting wearables to "see" more, farther and faster", *IEEE Access*, vol. 10, p. 29612-29632, 2022. doi: 10.1109/access.2022.3157876

[21] Y. Huo, F. Lu, F. Wu, & X. Dong, "Multi-beam multi-stream communications for 5g and beyond mobile user equipment and uav proof of concept designs", *IEEE 90th Vehicular Technology Conference*, 2019. doi: 10.1109/vtcfall.2019.8891154

[22] G. Arya, A. Bagwari, and D. S. Chauhan, "Performance analysis of deep learning-based routing protocol for an efficient data transmission in 5G WSN communication", in *IEEE Access*, vol. 10, pp. 9340-9356, 2022. doi: 10.1109/access.2022.3142082

[23] B. Shilpa, A. K. Budati, L. K. Rao, and S. B. Goyal, "Deep learning based optimized data transmission over 5G networks with Lagrangian encoder", *Computers and Electrical Engineering*, vol. 102, p. 108164, 2022. doi: 10.1016/j.compeleceng.2022.108164

[24] R. Ford, M. Zhang, M. Mezzavilla, S. Dutta, S. Rangan, and M. Zorzi, "Achieving ultra-low latency in 5G millimeter wave cellular networks", *IEEE Communications Magazine*, vol. 55, no. 3, pp. 196-203, 2017. doi: 10.1109/mcom.2017.1600407cm

[25] J. García-Morales, M. C. Lucas-Están, and J. Gozálvez, "Latency-sensitive 5G RAN slicing for industry 4.0", *IEEE Access*, vol. 7, pp. 143139-143159, 2019. doi: 10.1109/access.2019.2944719

[26] A. Hazarika and M. Rahmati, "Towards an evolved immersive experience: Exploring 5G-and beyond-enabled ultralow-latency communications for augmented and virtual reality", *Sensors*, vol. 23, no. 7, p. 3682, 2023. doi: 10.3390/s23073682

[27] G. Singh, S. Kumar, A. Abrol, B. K. Kanaujia, V. K. Pandey, M. Marey, and H. Mostafa, "Frequency reconfigurable quad-element MIMO antenna with improved isolation for 5G systems", *Electronics*, vol. 12, no. 4, p. 796, 2023. doi: 10.3390/electronics12040796

[28] O. P. Naser, H. G. Heba, H. M. Karim, H. S. Chan, R. A. A. A. Raed, N. M. A. Norah, "An efficient antenna system with improved radiation for multi-standard/multi-mode 5G cellular communications", *Sci. Rep*., vol. 13, p. 4179, 2023. doi: 10.1038/s41598-023-31407-z

[29] A. S. Alqahtani, S. B. Changalasetty, P. Parthasarathy, L. S. Thota, and A. Mubarakali, "Effective spectrum sensing using cognitive radios in 5G and wireless body area networks", *Computers and Electrical Engineering*, vol. 105, 2023. doi: 10.1016/j.compeleceng.2022.108493

[30] S. Y. Huang, H. H. Cho, Y. C. Chang, J. Y. Yuan, and H. C. Chao, "An efficient spectrum scheduling mechanism using Markov decision chain for 5G mobile network", *IET Communications*, vol. 16, no. 11, pp. 1268-1278, 2022. doi: 10.1049/cmu2.12263

[31] S. Grishma and S. Tappari, "Performance Analysis of 5G Waveforms for MIMO System," *Fifth International Conference on Electrical, Computer and Communication Technologies (ICECCT)*, pp. 1-6.,2023 doi: 10.1109/icecct56650.2023.10179661

[32] D. Anand, M. A. Togou, and G. M. Muntean, "A machine learning solution for video delivery to mitigate co-tier interference in 5G HetNets", *IEEE Transactions on Multimedia*, 2022. doi: 10.1109/tmm.2022.3187607

[33] C. Liu, Y. Xie, H. Li, Y. Wang, and Y. Zhang, "A Framework for Assessing the Resilience of 5G Mobile Communication Networks," *IEEE International Conference on Artificial Intelligence and Computer Applications (ICAICA)*, 2022, pp. 1077-1081. doi: 10.1109/icaica54878.2022.9844485

[34] R. Li, B. Decocq, A. Barros, Y. P. Fang, and Z. Zeng, "Estimating 5G network service resilience against short timescale traffic variation", *IEEE Transactions on Network and Service Management*, 2023. DOI: 10.1109/tnsm.2023.3269673

[35] S. Kaada, M. L. A. Morel, G. Rubino, and S. Jelassi, "Measuring 5G-RAN Resilience Using Coverage and Quality of Service Indicators," *IEEE/IFIP Network Operations and Management Symposium*, 2023, pp. 1-7. doi: 10.1109/noms56928.2023.10154368

[36] A. K. Sangaiah, A. Javadpour, P. Pinto, F. Ja'fari, and W. Zhang, "Improving quality of service in 5G resilient communication with the cellular structure of smartphones", *ACM Transactions on Sensor Networks (TOSN*), vol. 18, no. 3, pp. 1-23, 2022. doi: 10.1145/3512890

[37] V. Saravanan, P. Sreelatha, N. R. Atyam, M. Madiajagan, D. Saravanan, and H. P. Sultana, "Design of deep learning model for radio resource allocation in 5G for massive IoT device", *Sustainable Energy Technologies and Assessments*, vol. 56, p. 103054, 2023. doi: 10.1016/j.seta.2023.103054

[38] K. Koutlia, B. Bojovic, S. Lagen, X. Zhang, P. Wang, and J. Liu, "System analysis of QoS schedulers for XR traffic in 5G NR", *Simulation Modelling Practice and Theory*, vol. 125, p. 102745, 2023. doi: 10.1016/j.simpat.2023.102745

[39] Y. Zhang, H. Cao, M. Zhou, and L. Yang, "Spectral efficiency maximization for uplink cell-free massive MIMO-NOMA networks," *2019 IEEE International Conference on Communications Workshops (ICC Workshops)*, 2019, pp. 1-6. doi: 10.1109/iccw.2019.8756881

[40] S. Kusaladharma, W. P. Zhu, W. Ajib, and G. Amarasuriya, "Achievable rate analysis of NOMA in cell-free massive MIMO: A stochastic geometry approach," *IEEE International Conference on Communications (ICC)*, 2019, pp. 1-6. doi: 10.1109/icc.2019.8761506

[41] X. Hong, J. Wang, C. X. Wang, and J. Shi, "Cognitive radio in 5G: a perspective on energy-spectral efficiency trade-off", *IEEE Communications Magazine*, vol. 52, no. 7, pp. 46-53, 2014. doi: 10.1109/mcom.2014.6852082

[42] J. Wang, A. Jin, D. Shi, L. Wang, H. Shen, D. Wu, et al., "Spectral efficiency improvement with 5G technologies: Results from field tests", *IEEE Journal on Selected Areas in Communications*, vol. 35, no. 8, pp. 1867-1875, 2017. doi: 10.1109/jsac.2017.2713498

[43] S. M. Islam, M. Zeng, and O. A. Dobre, "NOMA in 5G systems: Exciting possibilities for enhancing spectral efficiency," *arXiv preprint* doi: 10.48550/arXiv.1706.08215

[44] A. L. Ha, T. H. Nguyen, T. Van, V. D. Nguyen, and W. Choi, "Deep learning-aided 5G channel estimation," *15th International Conference on Ubiquitous Information Management and Communication (IMCOM*), pp. 1-7.,2021. doi: 10.1109/imcom51814.2021.9377351

[45] H. A. Le, T. C. Van, T. H. Nguyen, H. Choo, and V. D. Nguyen, "Machine learning-based 5G-and-beyond channel estimation for MIMO-

OFDM communication systems", *Sensors*, vol. 21, no. 14, p. 4861, 2021. doi: 10.3390/s21144861

[46] M. Belgiovine, K. Sankhe, C. Bocanegra, D. Roy, and K. R. Chowdhury, "Deep learning at the edge for channel estimation in beyond-5G massive MIMO", *IEEE Wireless Communications*, vol. 28, no. 2, pp. 19-25, 2021. doi: 10.1109/mwc.001.2000322

[47] T. K. Vu, M. Bennis, S. Samarakoon, M. Debbah, and M. Latva-aho, "Joint Load Balancing and Interference Mitigation in 5G Heterogeneous Networks", *IEEE Transactions on Wireless Communications*, vol. 16, no. 9, pp. 6032-6046, 2017. doi: 10.1109/twc.2017.2718504

[48] Y. Wang, G. Feng, Y. Sun, S. Qin, and Y. C. Liang, "Decentralized learning based indoor interference mitigation for 5G-and-beyond systems", *IEEE Transactions on Vehicular Technology*, vol. 69, no. 10, pp. 12124-12135, 2020. doi: 10.1109/tvt.2020.3012311

[49] 3GPP TS 38.211 V15.5.0. Physical channels and modulation.*3rd Generation Partnership Project: Technical Specification Group Radio Access Network, 2018*

[50] 3GPP TS 38.211: V17.1.0. Physical channels and modulation. *3rd Generation Partnership Project: Technical Specification Group Radio Access Network,2022*

[51] M. Hijjawi, M. Shinwan, M. Qutqut, W. Alomoush, O. Khashan, M. Alshdaifat, A. Alsokkar, and L. Abualigah, "Improved flat mobile core network architecture for 5G mobile communication systems", *International Journal of Data and Network Science*, vol. 7, no. 3, pp. 1421-1434, 2023. doi: 10.5267/j.ijdns.2023.3.021

[52] L. Turchet and P. Casari, "Latency and Reliability Analysis of a 5G-Enabled Internet of Musical Things system", *IEEE Internet of Things Journal*, 2023. doi: 10.1109/jiot.2023.3288818

[53] A. A. El-Saleh, A. A. Abdulraqeb, S. Ibraheem, H. H. Wan, S. H. Mohamed, and I. D. Yousef, "Measurement analysis and performance evaluation of mobile broadband cellular networks in a populated city", *Alexandria Engineering Journal*, vol. 66, pp. 927-946, 2023. doi: 10.1016/j.aej.2022.10.052

[54] S. Lagen, B. Bojovic, K. Koutlia, X. Zhang, P. Wang, and Q. Qu, "QoS Management for XR Traffic in 5G NR: A MultiLayer System View and End-to-End Evaluation", *IEEE Communications Magazine*, 2023. doi: 10.1109/mcom.015.2200745

[55] A. Sufyan, K. B. Khan, O. A. Khashan, T. Mir, and U. Mir, "From 5G to beyond 5G: A Comprehensive Survey of Wireless Network Evolution, Challenges, and Promising Technologies", *Electronics*, vol. 12, no. 10, p. 2200, 2023. doi: 10.3390/electronics12102200

[56] S. Alraih, R. Nordin, A. A. Samah, I. Shayea, and N. F. Abdullah, "A Survey on Handover Optimization in Beyond 5G Mobile Networks: Challenges and Solutions", *IEEE Access*, 2023. doi: 10.1109/access.2023.3284905

[57] L. J. Horner, K. Tutschku, A. Fumagalli, and S. Ramanathan, "Virtual izing 5G and Beyond 5G Mobile Network", *Artech House*, 2023.

[58] R. Jayaraman, M. Baskar, S. Annamalai, M. Kumar, A. Mishra, and R. Shrestha, "Effective Resource Allocation Technique to Improve QoS in 5G Wireless Network", *Electronics*, vol. 12, no. 2, p. 451, 2023. doi: 10.3390/electronics12020451

[59]Watkins, Christopher JCH, and Peter Dayan. "Q-learning. ", *Machine learning* 8 , 279-292,1992. doi: 10.1007/BF00992698

[60] Patriciello, Natale. "5G new radio numerologies and their impact on the end-to-end latency.", *IEEE 23rd international workshop on computer aided modeling and design of communication links and networks (CAMAD)*. IEEE, 2018. doi: 10.1109/CAMAD.2018.8514979